

Far-infrared frequency dependence of the ac Josephson effect in niobium point contacts

D. A. Weitz,* W. J. Skocpol, and M. Tinkham

Department of Physics and Division of Applied Sciences, Harvard University, Cambridge, Massachusetts 02138

(Received 12 June 1978)

We have measured the far-infrared frequency dependence of the strength of the ac Josephson effect in Nb cat-whisker point contacts, which have consistent and reproducible behavior and minimal extrinsic high-frequency limitations due to capacitance and heating. We monitor the constant-voltage Josephson steps induced on the dc I - V curves by an optically pumped far-infrared laser at fundamental frequencies corresponding to voltages from ~ 0.2 to ~ 2 times the energy-gap voltage. At all the frequencies studied, we find that the shape of the power dependence of the step amplitudes is fit reasonably well by Werthamer's frequency-dependent theory for tunnel junctions in the voltage-bias approximation. However, the observed magnitude of the steps is considerably less than predicted by the theory. By fitting to the I - V curves of the steps, we find that some of this discrepancy can be accounted for by heating-enhanced noise rounding. The remaining discrepancies (of the order of a factor of 2) are attributed to departures from a voltage bias at low frequencies and, tentatively, to the effects of the Ginzburg-Landau relaxation time at higher voltages. Our data confirm the expected intrinsic roll off of the strength of the ac Josephson effect above the energy gap.

I. INTRODUCTION

The frequency dependence of the strength of the ac Josephson effect is of considerable interest, both as a fundamental question and in terms of the limitations it may place on potential applications. Although a wide variety of superconducting devices show the Josephson effect, the high-frequency behavior of many of these is dominated by such extrinsic limitations as capacitive shunting and Joule heating. These limitations can be minimized in niobium cat-whisker point contacts. Their minute size makes their capacitance very small,¹ while their three-dimensional geometry and relatively high impedance reduce heating effects.² We have identified a class of point contacts that are reproducible and consistent from junction to junction, both in the characteristic features on their dc I - V curves³ and in their high-frequency behavior,⁴ making them suitable for quantitative experiments. This has allowed us to measure the *intrinsic* frequency dependence of the strength of the Josephson effect.

We study the Josephson effect by monitoring the constant-voltage steps induced on the dc I - V curves by radiation from an optically pumped far-infrared (far-ir) laser. A fundamental step at a voltage V is direct evidence of the existence of the Josephson effect at the frequency $f = 2$ eV/h. By observing the power dependence of the current half-width of this step, we can study the strength of the Josephson effect at that frequency. In particular, by measuring the *maximum* current half-width of the fundamental step normalized to the critical current,⁵ $I_{1/2}^{\max}/I_c$, at

various laser wavelengths, we can determine the far-ir frequency dependence of the Josephson effect.

The theoretical predictions for the frequency dependence of the strength of the Josephson effect and the power dependence of the step current widths are discussed in Sec. II of this paper. Section III is a brief description of our experimental techniques. Our measurements are presented in Sec. IV, along with a discussion of the effects of heating and noise on both the size and the shape of the steps. The frequency dependence of the Josephson effect inferred from these measurements is discussed in Sec. V.

II. THEORY

Our ability to measure the strength and frequency dependence of the Josephson effect depends on a study of the laser-induced constant-voltage steps on the dc I - V curves. Thus, we need a theoretical model to relate the behavior of the steps to that of the Josephson effect itself. In this section, we discuss the theoretical predictions that we fit to our measurements of the power dependence of the laser-induced steps.

The ill-defined geometry and physical structure of the active region make the choice of an appropriate theoretical mode of point contacts extremely difficult. None of the theories currently available adequately describes the characteristic shape of the dc I - V curves of our junctions.^{3,5} Thus, the accuracy of their prediction of the shape of the constant voltage steps and their power dependence may be somewhat questionable.

In order to make the calculations more tractable, all of the theories make simplifying approximations for the source impedance. They assume either a low-resistance constant-voltage source, or a high-resistance constant-current source. Experimentally, the bias impedance lies somewhere in between, and probably has a rather complicated frequency dependence as well. The dc source impedance is defined by the bias network used. In these experiments, it was always very high compared to the junction resistance R . However, we have shown⁴ that the rf source impedance seems to be that of the antenna, and is $\sim 200 \Omega$ at 604 GHz. This is not much larger than the resistance of a typical junction ($R \sim 100 \Omega$). The type of bias network assumed can have a significant effect on the theoretical predictions. Unfortunately, a tractable model with a more realistic bias impedance does not exist.

Some of the theoretical calculations of the step power dependences are based on a tunnel-junction model of the weak link. Experimental evidence seems to suggest that our point contacts are better described as extremely small metallic constrictions.³ Nevertheless, tunnel-junction models often seem to work quite well for point contacts, and give good qualitative agreement with much of the data. The reproducibility of our measurements allows us to test the theories more quantitatively.

The current I , through a small-area junction at temperature T and bias voltage V , can be written⁶

$$I = I_p(V, T) \sin \phi + I_{qp}(V, T) + I_{qpP}(V, T) \cos \phi, \quad (1)$$

where

$$\frac{d\phi}{dt} = \frac{2eV}{\hbar}, \quad (2)$$

and ϕ is the phase difference across the tunnel junction. The actual expressions for the coefficients in Eq. (1) depend on the type of model assumed, as discussed below. The first term is the supercurrent or Josephson pair current, and at low frequencies (voltages) $I_p \approx I_c$. The second term is the quasiparticle or normal current, which is highly nonlinear in the case of a tunnel junction. The linear approximation of a constant resistance R leads to the resistively shunted junction (RSJ) model, with $I_{qp} = V/R$. The final term is the cosine term, and has no effect on the magnitude of the steps for a voltage-biased junction.⁷ It is usually omitted in the RSJ approximation.

The simplest approximation for the power dependence of the step current widths is obtained for low frequencies (so that $I_p = I_c$) and for a junction voltage biased with both a dc voltage V_0 and a laser-induced ac voltage of angular frequency ω_L , $V_{ac} \cos \omega_L t$. This results in the familiar Bessel-function power dependence of the steps,⁸

$$I_n/I_c = |J_n(2\alpha)|, \quad (3)$$

where

$$2\alpha = 2eV_{ac}/\hbar\omega_L. \quad (4)$$

Here J_n is the n th Bessel function and I_n is the current half-width of the n th step at the dc voltage

$$V_0 = n(\hbar\omega_L/2e). \quad (5)$$

Werthamer⁹ has calculated the voltage (frequency) dependence of Eq. (1) at $T=0$, assuming a perfect BCS density of states for the superconductors on either side of the barrier. The results for the supercurrent I_p can be written¹⁰

$$I_p(\omega_J) = \frac{2}{\pi} I_c \begin{cases} K(\hbar\omega_J/4\Delta), & \hbar\omega_J/4\Delta \leq 1 \\ \frac{4\Delta}{\hbar\omega_J} K(4\Delta/\hbar\omega_J), & \hbar\omega_J/4\Delta \geq 1 \end{cases}, \quad (6)$$

where ω_J is the Josephson frequency [or voltage $V = (\hbar/2e)\omega_J$], 2Δ is the superconducting energy gap energy, and K is the complete elliptic integral of the first kind. According to Eq. (6), the Josephson current is approximately constant at voltages below the gap, has a logarithmic singularity (the Riedel peak¹¹) at the gap, and falls off approximately as $1/\omega_J$ above the gap. When this frequency dependence of I_p is included, Eq. (3) is generalized to¹⁰

$$\frac{I_n}{I_c} = \left| \sum_{k=-\infty}^{\infty} J_k(\alpha) J_{n-k}(\alpha) I_p(|2k-n|\omega_L) \right|. \quad (7)$$

If the summation converges before $|2k-n|\omega_L$ becomes comparable to $4\Delta/\hbar$, Eq. (7) reduces to the simple Bessel-function dependence of Eq. (3). Thus at low ac frequencies, the effect of the frequency dependence of I_p is not seen until α becomes quite large,¹⁰ requiring large rf drive powers. However, for the relatively high laser frequencies used in this experiment, Eq. (7) must be used for all laser powers.

If one of the $|2k-n|\omega_L$ harmonics of the laser frequency is equal to $4\Delta/\hbar$, that term in the summation in Eq. (7) becomes singular. This has a pronounced effect on the power dependence of the step, and has been used to experimentally study the Riedel singularity in tunnel junctions,^{10,12} point contacts,¹³ and microbridges.¹⁴ The maximum step width enhancement due to the singularity is generally found to be about a factor of three. To obtain quantitative agreement with the data, the theory must be modified to account for mechanisms such as quasiparticle damping,¹⁵ which round off the singularity. This adds a complex component to the energy gap parameter $\Delta(\omega)$, which must be included in a modified version of Eq. (7). This has been done by Buckner and Langenberg,¹² who find good agreement between their theoretical calculations and their tunnel-junction data.

All the experimental investigations to date have measured the frequency dependence of I_p only in the

vicinity of the singularity. Thus they have been restricted to a frequency range within $\sim 5\%$ of the Josephson frequency at the gap, $\omega_J = 4\Delta/\hbar$. Our experiment is not designed to probe the singularity. In fact, we have not found it necessary to use the rounded-singularity version of Eq. (7) to account for any of our data. Instead, we wish to extend the frequency range of the measurement, particularly above the gap.

Examination of Eq. (7) clearly shows why the fundamental laser-induced steps are the most direct probe of the strength of the Josephson effect above the energy-gap frequency. For $n = 1$, the leading term in the summation is

$$2J_0(\alpha)J_1(\alpha)I_p(\omega_L) ,$$

which is the contribution from the Josephson current at the laser frequency. The additional terms are contributions from I_p at higher harmonics of ω_L , where the Josephson current has rolled off even further. In contrast, for a step at a harmonic of a lower frequency, there is always a contribution to the summation from $I_p(0)$ for n even, and from $I_p(\omega_L)$ for n odd. These terms add a lower-frequency component of the Josephson current, where I_p is larger. Thus, a harmonic step is a less direct measure of $I_p(n\omega_L)$ than the fundamental step at the same voltage. In our experiments, we vary the laser wavelength and use only the fundamental step to study the frequency dependence of the Josephson effect.

Both theories resulting in Eqs. (3) and (7) make the approximation of a purely voltage bias at all frequencies. Other models make the opposite approximation for the source impedance, treating the junction as current biased. The simplest of these is the current-biased RSJ model,¹⁶ in which $I_p(\omega) = I_c$, $I_{qp} = V/R$, and $I_{qp,p} = 0$. Russer¹⁷ has used an analog computer to calculate the RSJ predictions of the power dependences of the steps for various normalized frequencies,

$$\Omega = \hbar\omega_L/2eI_cR . \quad (8)$$

He finds that the Bessel-function behavior predicted by Eq. (3) is a good approximation for $\Omega > 1$, but that substantial changes due to the current bias occur when $\Omega < 1$. At low temperatures, I_cR is theoretically¹⁸ related to the gap voltage by

$$I_cR = \frac{1}{4}\pi 2\Delta/e . \quad (9)$$

Thus, we expect a current bias to cause significant changes in the power dependence when the fundamental step is below the gap voltage.

While the RSJ model gives a qualitative account of the influence of a current bias, it does not include any effects due to the frequency dependence of the Josephson current. To do this, we must use the full frequency-dependent theory⁹ itself, inverting Eq. (1)

in order to solve for the voltage, with the assumption of a current bias.¹⁹ This is simplified by the use of a reformulation of the theory in the time domain.²⁰ It includes the full frequency dependence of the Josephson current, as well as any effects the cosine term may have for the current-biased case. However, unlike the RSJ model, the quasiparticle term includes the nonlinear resistance characteristic of a tunnel junction.

We have performed computer calculations, using a technique similar to that suggested by Harris,²¹ to determine the step widths for the cases of both dc and ac current sources. The current and voltage across the junction are assumed to be zero until time $t = 0$, when the current drives are switched on. Then the Werthamer theory in the time domain is used to calculate the voltage across the junction, with the results at each time depending on the voltage at all previous times. The calculation is carried on until the transient effects,²⁰ due to the initial change in drive currents, die out. Figure 1 shows an example for $\hbar\omega_L/4\Delta \approx 0.45$, the normalized energy of the 496- μm laser line (assuming a superconducting gap energy of 2.8 mV). Both the instantaneous voltage (solid line) and the average voltage (dashed line) are plotted as functions of time. Figure 1(a) is for a junction biased on the first laser-induced step, so that the current is periodic at the laser frequency, and the average voltage is approaching the constant value of 1.25 mV ($0.45 \times 2\Delta/e$). Figure 1(b) shows similar results for a dc bias *not* on a step. In this case the voltage is not periodic, and the average voltage is approaching $\sim 0.65(2\Delta/e)$, intermediate between the first and second steps. By monitoring quantities such as these, it is possible to determine whether or not the junction is biased on a step, for given levels of dc and ac currents. Then, by tracing out the dc bias currents that put the junction on a step, the current width of the step can be determined. This process is repeated for successively increasing laser powers to find the power dependence of the current width. Unfortunately this requires considerable computer time, so we have made only limited use of these calculations.

We have discussed four models that predict a power dependence for the step current widths. Two of them make the assumption of a voltage bias, the other two assume a current bias. One of each type of bias includes the frequency dependence of the Josephson effect, the other does not. We now compare these theoretical models to our data.

III. EXPERIMENTAL TECHNIQUES

The experiments were performed using point contacts formed between a 75- μm -diam. Nb wire, sharpened to a fine point with standard electroetching techniques,²² and a polished and lightly etched Nb

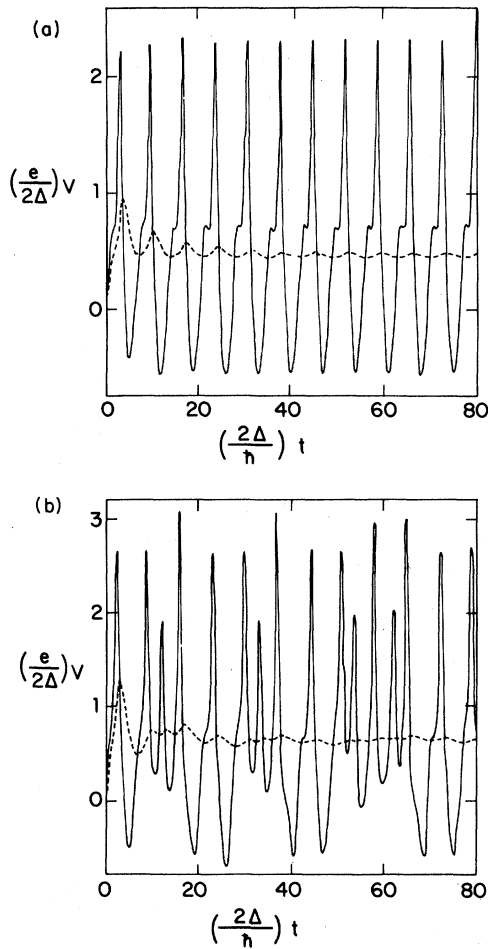


FIG. 1. Results of computer calculations using the frequency-dependent theory for a junction with ac and dc current biases. The ac source has a magnitude of $0.5(2\Delta/eR)$ and a frequency of $0.90(2\Delta/\hbar)$. Both the instantaneous (solid lines) and the time-average (dashed lines) voltages are shown. The dc bias level is (a) on the step, so the average voltage is approaching $0.45(2\Delta/e)$, and (b) between the first and second steps, so the average voltage is approaching $0.65(2\Delta/e)$.

flat. The contact was made while the junction was immersed in liquid helium. A technique³ that involved fine mechanical adjustment and a high current burn-in was found to be quite successful in obtaining high quality junctions. Only those junctions that showed a strong Josephson effect at high voltages³ and whose dc I - V curves had the characteristic shape we have labeled "ideal,"⁵ were used in this work. A high impedance battery-driven source supplied the dc current bias, and the voltage was measured directly across the junction with a PAR 113 differential preamplifier. All the leads were brought through rf filters at the top of the metal Dewar to minimize spurious pick up.

An $\sim f/4$ polyethylene lens focused the far-ir laser radiation onto the contact through two crystal quartz windows in the side of the Dewar. A bend in the whisker defined a ~ 500 - μm -long antenna to couple the radiation into the junction. The contacts used had typical resistances of $\sim 100 \Omega$, and thus were well matched to the antenna and to free space.⁴ The optically pumped far-ir laser used has been described in detail elsewhere.²³ It could be operated at wavelengths from $42 \mu\text{m}$ to 1.22 mm , with about 10-mW typical output power on the stronger lines. The wavelengths and gases used in this work were: 1.22 mm (245 GHz) from $^{13}\text{CH}_3\text{F}$, $496 \mu\text{m}$ (604 GHz) from $^{12}\text{CH}_3\text{F}$, $233 \mu\text{m}$ (1.29 THz) from N_2H_4 , and $202 \mu\text{m}$ (1.48 THz), $170 \mu\text{m}$ (1.76 THz), and $119 \mu\text{m}$ (2.52 THz), all from CH_3OH .

IV. DATA ANALYSIS

A. Power dependence of step current widths

Our initial results⁴ were obtained using the 496 - μm line, which produced a fundamental step at 1.25 mV , somewhat less than half the gap voltage. When the data were scaled to account for the coupling efficiency, the behavior of I_n/I_c was very reproducible from junction to junction. Figure 3 of Ref. 4 is a composite plot of data from five different junctions of varying resistances. It shows the power dependence of I_n/I_c for the critical current and the first eight steps ($n=0$ to $n=8$). The shape of the power-dependence data was reasonably well described by the Bessel-function prediction of Eq. (3). Even better agreement was obtained when the frequency-dependent effects of Eq. (7) were included. However, the magnitudes of the experimentally observed steps were consistently at least a factor of 2 smaller than expected from either calculation. A possible cause for this discrepancy is the effect of a current bias. Indeed, the current-biased RSJ model does predict a reduction in the step size in approximate agreement with that observed. However, Ω is large enough (~ 0.6 for a typical $I_c R$ of 2.0 mV) so that the shape of the current-biased RSJ curves does not differ significantly from the voltage-biased Bessel-function behavior of Eq. (3). Thus we can not convincingly distinguish between the two models using the shape of the data.

If the data were better described by a current-bias model, the improvement should become more pronounced at lower Ω .¹⁷ To check this, we went to a lower frequency, using the 1.22 -mm line, which induces a fundamental step at 0.51 mV , so that $\Omega \approx 0.25$. Figure 2 shows the power dependence of I_n/I_c for the critical current and the first six steps. The normalized voltage amplitudes on the horizontal axis have been obtained by scaling all of the data for a given point contact by a single factor, which depends on its coupling efficiency. The shape

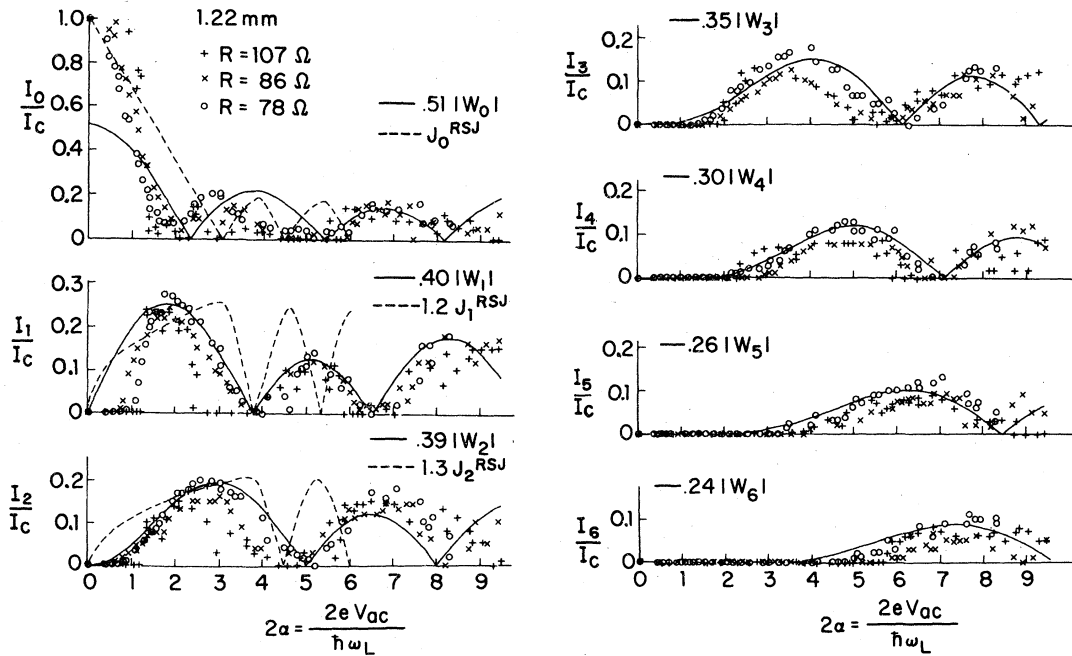


FIG. 2. Normalized step width behavior as a function of 1.22-mm laser-induced voltage, compared to the frequency-dependent, voltage-bias Werthamer theory and current-bias RSJ model. This is a composite plot with data from three different junctions.

predicted by Eq. (7) is shown by the solid lines (W functions) in Fig. 2, and is in reasonably good agreement with the data for steps 1–6, although the theoretical step size must be scaled down by the factors indicated in Fig. 2 to obtain quantitative agreement. In contrast, the current-biased RSJ prediction does not do as well. It predicts a step size even smaller than observed and predicts a shape of the power dependence, shown by the dashed lines (J^{RSJ} functions) in Fig. 2, which is quite different from that observed. Thus it appears that the well matched source impedance of the antenna⁴ is better described by a voltage-bias model in predicting the shape of the power dependence.

Neither theory adequately describes the behavior of the critical current (zeroth step). The first zero occurs at significantly lower power levels than expected from the current-biased RSJ model. On the other hand, the amplitude of the critical currents beyond the first zero is much smaller than predicted by the voltage-biased Werthamer theory, unless it is scaled so that it fails to agree at zero power. Similar disagreements were observed with the 496- μm data. The reason for this poor agreement is not known, although it is likely related to the peculiar behavior of the I - V curves in the vicinity of the critical current that is always seen when these junctions are irradiated by low levels of laser radiation.²⁴ The effect of the radiation is not only to decrease I_0 , but also to decrease substantially the initial dynamic resistance of the voltage onset, changing it from the very steep on-

set seen without incident radiation, to a much more gradual one. This behavior is seen for all the laser frequencies we have investigated.

Comprehensive data such as that obtained at 1.22 mm and 496 μm could not be obtained at the other far-ir wavelengths used. These laser lines are all much higher in frequency, with the corresponding fundamental steps at voltages near, or well above, the energy gap. Thus there are fewer observed harmonics to fit to the theory. In fact, for the remaining frequencies, the second step was generally very small, and the higher harmonics were usually not seen at all. Furthermore, at these frequencies we were unable to couple in enough power to reach the same high values of

$$2\alpha = 2eV_{\text{ac}}/\hbar\omega_L$$

that were reached at the lower frequencies. Operating at 496 μm , the laser power (measured at the laser output coupler) was ~ 10 mW, sufficient to obtain $2\alpha \approx 12$. However, 2α scales as V_{ac}/ω_L , so that the power ($\sim V_{\text{ac}}^2$) required to reach the same 2α scales as ω_L^2 . Thus, even though the output power at 119 μm was ~ 80 mW, we would expect to reach values of 2α of only ~ 5.5 . In fact, our optics were considerably more lossy at 119 μm than at 496 μm , and the coupling to the antenna may not have been as good, so that we were only able to reach $2\alpha \sim 3$.

As a result of the low values of 2α attained and the associated lack of observed harmonics, there was insufficient structure in the power-dependence data to

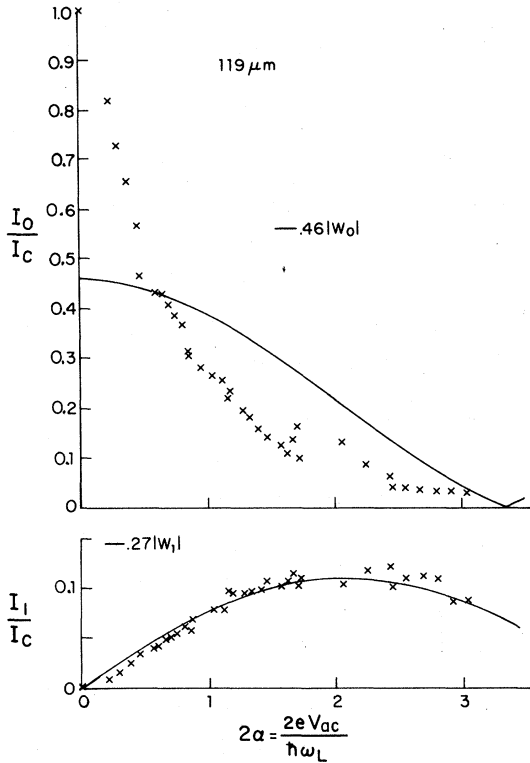


FIG. 3. Normalized step width behavior as a function of 119- μm laser-induced voltage, compared to the frequency-dependent voltage-bias Werthamer theory.

obtain a convincing fit to the theory. Figure 3 shows the power dependence of I_0/I_c and I_1/I_c for a typical junction exposed to 119 μm radiation, and their fit to the scaled shape of the voltage-bias theory of Eq. (7). As with the lower frequencies, the low laser-power behavior of I_0 resulted in a poor fit to the theory. Following the example of the fit to the data of frequencies below the gap, the theoretical calculation of I_0/I_c is scaled by ~ 0.5 in Fig. 3. The only reliable structure in the data that is useful for a fit to the theory is the first hump of I_1 .

We also attempted similar measurements using the 71 μm line of CH_3OH . However, there was not enough laser power available to see the first step at 8.75 mV. The ω_L^2 dependence of the power required means that a factor of ~ 3 increase in power over that available at 119 μm is necessary to reach comparable values of 2α for equal coupling efficiencies. However, both the losses in the optics and the attenuation in atmosphere are quite severe at 71 μm . Thus, although we estimate that we had at least several milliwatts of power at 71 μm , this was not sufficient with the coupling scheme used.

When the data at all the wavelengths are considered as a whole, the voltage-bias theory of Eq. (7) appears to give quite reasonable agreement with the

shape of the data. The reason for the discrepancy between the observed step size and that predicted must still be explained. Since the frequencies involved are so high, we have investigated the effects of a small shunting capacitance on the predicted step size. The addition of a capacitive rolloff has little effect on the power dependences calculated with Eq. (7), so long as $(RC)^{-1}$ is greater than the gap frequency. Larger values of capacitance remove the benefits of including the frequency dependence and give a poorer fit to the 496- μm data. Smaller values do not cause any reduction in the predicted step widths. We have also used an analog simulator²⁵ to calculate the power dependences within the RSJ model with the addition of a small shunting capacitance. We again find no reduction in the step sizes. Thus, the evidence available suggests that the capacitance is indeed small enough to neglect entirely. We now consider other effects that might reduce the step size.

B. Heating

Heating has been proposed as a mechanism which reduces the critical current, and hence the step widths. Tinkham *et al.*² have treated in detail the case of a metallic junction of the point-contact geometry. They find an exponential decrease in the step widths as the total dissipated power P is increased, with

$$I_n \propto e^{-P/P_0}, \quad (10)$$

where P_0 is predicted to be $\sim 10 \mu\text{W}$ for a typical metallic Nb point contact. We can calculate P for a given laser power using the good fit of the power dependences of the step widths to the voltage-bias model to obtain the normalized laser-induced voltage in the junction 2α . Combining this with the power dissipated by the dc bias current

$$P = P_{\text{dc}} + P_{\text{ac}} = V^2/R + (\hbar\omega_L/2e)^2(2\alpha)^2/2R. \quad (11)$$

For a typical 100- Ω junction biased at the 5.22-mV step induced by 119- μm radiation, Eq. (11) gives $P \approx 1.5 \mu\text{W}$ for $2\alpha = 3$, the maximum value reached in these experiments. For the eighth harmonic induced by 496- μm radiation at 10 mV, $P \approx 2 \mu\text{W}$ for $2\alpha = 12$. These values of P suggest that heating will have only a small effect, mainly on the high-voltage steps, at higher laser-induced powers. It should cause a maximum reduction in the step size of only $\sim 20\%$. We now present further evidence supporting this.

The very pronounced gap structure on the I - V curves can be used as a local thermometer to measure the temperature T , roughly a coherence length ξ away from the center of the active region of the point

contact.²⁶ The laser-induced Josephson steps can obscure this structure unless the voltage of the first step is above the gap voltage. It is then possible to measure the rise in temperature over the bath $T - T_b$ due to the laser-induced power, which is determined using Eq. (11) and the power-dependence fit of the step widths. Figure 4 shows $T - T_b$ due to the total dissipated power for increasing levels of 170- μm radiation. The width of the gap structure makes it difficult to determine an exact gap voltage, especially at higher laser powers, where the shape becomes somewhat less pronounced. This leads to considerable scatter in the data of Fig. 4. The gap voltage was taken as the voltage of the minimum R_D in the gap structure. The corresponding temperatures T were obtained from the measured temperature dependence of the energy gap of Nb-Nb tunnel junctions,²⁷ which have low-temperature gap voltages in good agreement with those of our point contacts.

Using Fig. 4, we can obtain a measure of some of the experimental parameters important in the heating theory. In the low heating limit, Tinkham *et al.*² find that

$$T - T_b = P / \Omega K \xi, \quad (12)$$

where K is the thermal conductivity, and Ω is the effective solid angle for the three-dimensional cooling

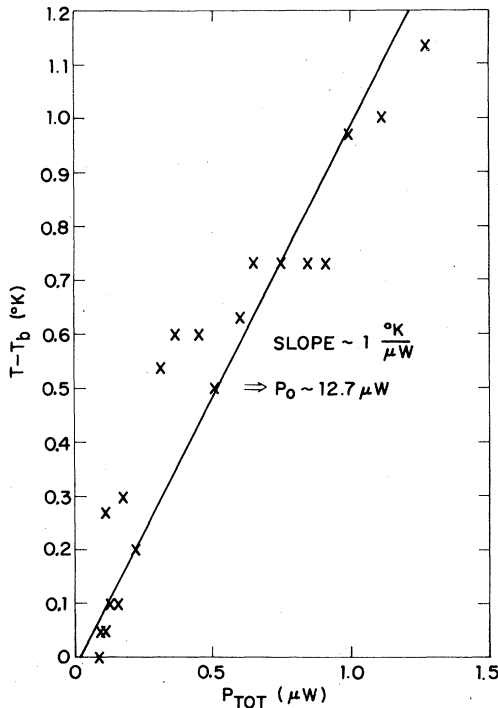


FIG. 4. Temperature rise a coherence length away from the contact as the dissipated power is increased with 170- μm laser radiation. The gap voltage is used as a local thermometer.

of the active region of the contact. From the slope of the solid line in Fig. 4, $\Omega K \xi \approx 1 \mu\text{W/K}$. These are the only unknown quantities in the expression for P_0 ,

$$P_0 = (1/\sqrt{2})(1 - t_b^2)^{1/2} K(T_c) T_c \xi(0) \Omega, \quad (13)$$

where $t_b = T_b/T_c$. Using the temperature dependences, $K \propto T$ and $\xi \propto (1 - T/T_c)^{-1/2}$, and $T_c \approx 9.2$ K for Nb, Eq. (13) and the measured $K \Omega \xi$ give $P_0 \sim 12 \mu\text{W}$. While this is only an approximation and should not be taken as an exact measure of P_0 , it is nevertheless consistent with the predictions of the theory.

Other evidence also supports the hypothesis that these junctions are operating in the low heating limit. As shown in Fig. 4, the maximum increase in temperature a coherence length away from the contact is only ~ 1 K, which should not have a major effect on the supercurrent. We also find very consistent behavior of the normalized step widths for junctions whose resistances vary between ~ 30 and 200Ω , while the dissipated power is proportional to $1/R$. Thus we believe that heating causes at most only a $\sim (10-20)\%$ reduction in the step widths, illustrating the well cooled nature of these point contacts.

C. Noise

Fluctuations in the phase due to noise can have an important effect on the shape of the step, causing the edges to be rounded and the dynamic resistance of the step center to be greater than zero.²⁸ This can have a significant effect on the measured current width of the step. The only available detailed theoretical treatment of the effects of noise on the shape of the step is within the RSJ model. Within this approximation, the unrounded step has the same characteristic hyperbolic shape as the dc I - V curve.

Since the dc I - V curve of our junctions is so highly structured, it is quite likely that the unrounded step shape is also more complicated than the relatively structureless RSJ prediction. In fact, the measured step shape seems to depend on where it is on the I - V curve. Figure 5 shows the shape of the fundamental step induced by a number of different far-ir laser wavelengths at various voltages. The steps are superimposed on a typical dc I - V curve with no incident radiation. Although each step is from a different junction, all the dc I - V curves have the same characteristic shape and the current width of each step shown is normalized to its own I_c . Figure 5 shows how the step shape seems, in some sense, to mimic the underlying structure on the dc I - V curve at that voltage. The 0.5-mV step (1.22-mm radiation) occurs on the very steep initial voltage rise, and the sides of the step also show this high dynamic resistance R_D . The steps at 1.25 mV (496 μm), 3.65 mV (170 μm), and 5.22 mV (119 μm) all occur on portions of the I - V curve that do not have a lot of extra structure or

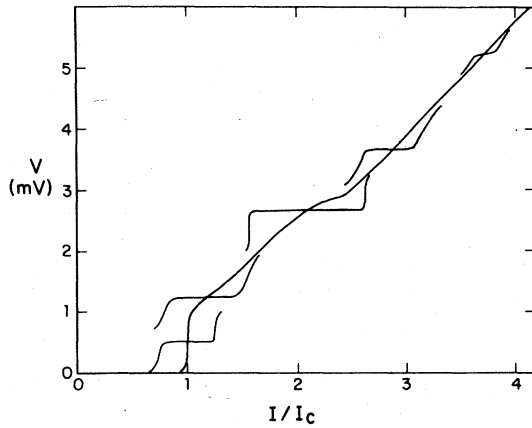


FIG. 5. Variation in the shape of the step with its voltage. Each step is taken from a separate high quality I - V curve and its width is normalized to its own I_c . They are superimposed on a typical I - V curve to show the underlying shape.

high R_D , and these steps all have shapes somewhat closer to that of the RSJ model. The step at 2.64 mV occurs on the gap structure and is enhanced due to the effects of the Riedel peak. Its shape is quite different from the other steps and has a very large dynamic resistance on either side. Thus, the adequacy of the RSJ model in describing the shape of the step depends somewhat on the voltage of the step.

Despite the highly structured shapes of the experimentally observed steps, the RSJ model is still a reasonable first approximation, especially for a description of the effects of noise rounding. We have fitted the theoretically predicted shape²⁸ to the measured one in an attempt to evaluate and correct for the effects of noise rounding. The predicted shape of the n th step can be written²⁹

$$v_1 = \frac{1}{2} R_D i_0 \sinh(\pi i_1 / i_0) \times \left(\int_0^{\pi/2} \cosh(2y i_1 / i_0) I_0(2I_n / i_0) \cos y \, dy \right)^{-1}, \quad (14)$$

where

$$i_0 = 2ek_B T_{\text{eff}} R_D I / \hbar V.$$

Here I , V , and R_D are, respectively, the current, voltage, and dynamic resistance at the step center in the absence of radiation, while i_1 and v_1 are, respectively, the current and voltage along the induced step, measured from its center. I_0 is the modified Bessel function. The effective noise temperature T_{eff} is not the bath temperature, because of the heating in the point contact.^{2,4,24} Thus, we must use a two parameter fit in T_{eff} and I_n , the current half-width of the step in the absence of noise rounding.

The value of the parameter $R_D I / V$ in Eq. (14)

depends on the position of the step on the I - V curve. Within the RSJ model, this takes account of the underlying shape of the dc I - V curve. At low step voltages, where the underlying R_D is larger, the effects of noise should be more pronounced. On our I - V curves, $R_D I / V \sim 1$ for all the steps except the one induced by 1.22-mm radiation at 0.51 mV. In the latter case the fit to the RSJ model is poor and gives no evidence of enhanced noise rounding.

An example of the type of fit we obtain is shown in Fig. 6. The data, shown as the crosses, are the fourth harmonic of the 496- μm , laser-induced step at 5.0 mV, and the experimentally measured current half-width of the step was 2.1 μA . The solid lines are the calculated step shapes using Eq. (14). The fits shown in each figure use the indicated value of

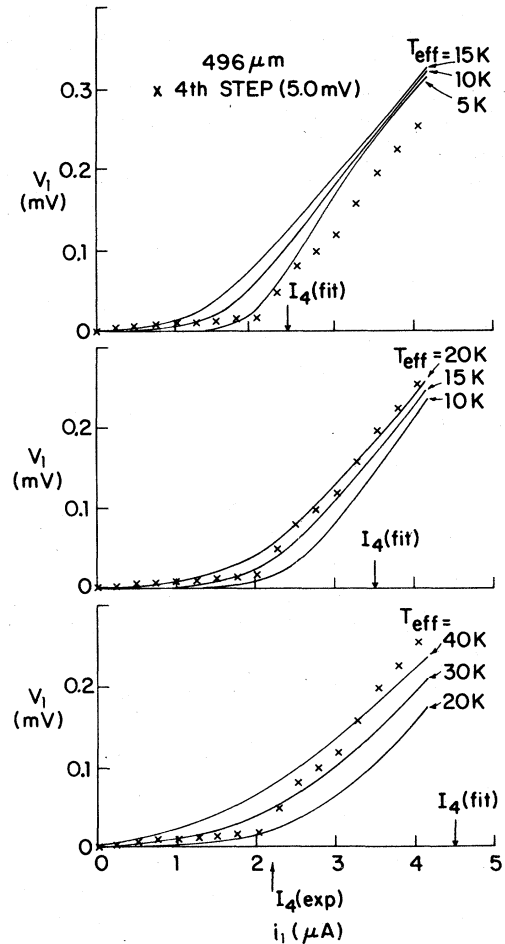


FIG. 6. Two parameter fit for the effects of noise rounding. The crosses are data showing the 4th step, at 5.0 mV, induced by 496- μm radiation. The solid lines are the calculated noise-rounded RSJ shape using Eq. (14) in the text. Each figure is for a different fitting value of I_4 , the unrounded step width, and shows the shape for three effective noise temperatures.

I_4 , and are calculated for various values of T_{eff} . The best fit is for $I_4 \sim 3.5 \pm 0.5 \mu\text{A}$ and $T_{\text{eff}} \sim 15 \pm 5 \text{ K}$. The accuracy of the fit is sufficient to obtain a reasonable correction to the step widths to account for the effects of noise rounding. As shown by the example in Fig. 6, these corrections can be quite substantial.

V. FREQUENCY DEPENDENCE OF THE JOSEPHSON EFFECT

Using the results of the last section, the frequency dependence of the Josephson effect can be determined. As discussed in Sec. II, we use the results from the fundamental step, which is most closely related to the strength of the Josephson effect at that frequency (voltage). Figure 7 is a plot of I_1^{max}/I_c as a function of voltage, normalized to the gap voltage $2\Delta/e$ for all of the laser lines used.³⁰ The large dots represent the largest values of I_1^{max}/I_c actually measured, while the error bars represent the range of values after corrections have been made for the effects of noise rounding and heating as described in the previous section. The vertical error bars represent the uncertainty in the noise-rounding fit, while the horizontal error bars represent the uncer-

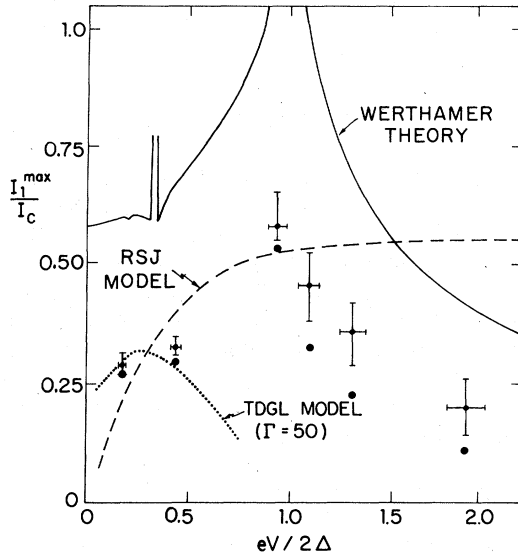


FIG. 7. Voltage dependence of the ac Josephson effect. The maximum width of the fundamental Josephson step normalized to the critical current is plotted against the step voltage normalized to the energy gap. The dots represent the measured data, while the error bars represent the range of values after they are corrected for the reductions due to noise and heating. The horizontal error bars reflect the uncertainty in the energy-gap voltage. The solid curve is the voltage-bias Werthamer theory result; the dashed curve is the current-bias RSJ result; and the dotted curve is the TDGL result from Ref. 34.

tainty in the exact voltage of the energy gap, reflecting the width of the structure on the dc I - V curve. We had enough laser power to reach the maximum of I_1 for all of the steps except the one at $eV/2\Delta \approx 1.1$ ($202 \mu\text{m}$). The datum shown for this frequency is an estimate of I_1^{max}/I_c obtained from a fit of Eq. (7) to the available power-dependence data, and is thus a somewhat less accurate result (hence the larger error bars on the corrected value).

The solid line in Fig. 7 is the prediction of the voltage-bias, frequency-dependent theory calculated with Eq. (7). The singularities at the gap and at one third of the gap would be rounded off, but the details of this would depend on the experimental conditions. The data follow the shape of the theory, peaking near the gap and rolling off above the gap. However, the magnitude of the data is consistently below that of the theory, even after the adjustments for noise rounding and heating are made.

Below the energy gap, a reduction in I_1^{max}/I_c is expected if the junction is current-biased rather than voltage-biased. The dashed line in Fig. 7 shows the reduction expected within the RSJ model. We have also investigated the effects of a current bias on the prediction of the frequency-dependent theory at a voltage $eV/2\Delta \approx 0.45$, corresponding to the $496\text{-}\mu\text{m}$ laser-induced step. Using the computer calculations described in Sec. II, we obtain $I_1^{\text{max}}/I_c \approx 0.35$, which is in good agreement with the experimental value. Thus it is tempting to attribute the decrease simply to current-bias effects. However, as shown in Sec. IV A, this is not completely justified. At $eV/2\Delta \approx 0.18$ (1.22-mm line), where the effect of a current bias should be more pronounced, the measured I_1^{max}/I_c is larger than predicted by the RSJ model, and the shapes of the step power-dependences are better described with a voltage-bias approximation.

Although a current-bias approximation predicts a decrease in I_1^{max}/I_c below the gap, the RSJ curve rapidly converges above the gap on the simple voltage-bias prediction of Eq. (3), $I_1^{\text{max}}/I_c \approx 0.58$, as shown in Fig. 7. Thus the effects of a current-bias approximation cannot explain the discrepancy between the data and the theory above the gap, although a more realistic handling of the source impedance might improve the agreement.

An alternative explanation of this discrepancy above the gap is the possible existence of a more rapid rolloff than predicted by the Werthamer theory. At these high frequencies, the Josephson period is shorter than the Ginzburg-Landau time

$$\tau_{\text{GL}} = \pi \hbar / 8 k_B (T_c - T) ,$$

and this may affect the dynamics of the currents in the junction and cause the smaller steps. The effects of a nonzero value for τ , the order-parameter relaxa-

tion time, have been examined^{31,32} using time-dependent Ginzburg-Landau (TDGL) theory, and offer a possible explanation of the excess current characteristic of our dc I - V curves. Fjordbøge and Lindelof³³ have recently used an analog computer to solve the relevant TDGL equations with the addition of an rf current source. The normalized parameter that determines the extent of the nonequilibrium effects in this formulation is

$$\Gamma = \tau(2eI_c R / \hbar)(a/\xi)^2.$$

Here, a is the length of a metallic bridge whose massive banks are assumed to be unaffected by any nonequilibrium effects ("rigid" boundary conditions). The calculated³³ I_1^{\max}/I_c for $\Gamma = 50$ (the only value reported) is shown as a dotted line in Fig. 7. This prediction is consistent with the slight increase in the step size over the RSJ prediction at low frequencies in agreement with 1.22-mm data. At higher frequencies, it shows that the effects of a nonzero τ will indeed cause a more rapid rolloff in the strength of the Josephson effect. For the value of Γ shown here, the predicted rolloff is much more rapid than what is measured. However, the shape of our high quality I - V curves, in particular the excess-current region above the gap, is best described³ by TDGL calculations using $\Gamma \approx 6$, which is the value that corresponds to $\tau \approx \tau_{GL}$ and $a/\xi = 1$. Presumably, as Γ is decreased, the nonequilibrium effects will diminish and the TDGL result will begin to resemble the RSJ prediction. This should have the effect of pushing the rolloff of I_1^{\max}/I_c to higher frequencies, in better agreement with the data. Thus further calculations with the TDGL theory at smaller values of Γ may provide a better fit to the data. Such a theory alone, however, does not include the singular behavior at the gap frequency suggested by our data and other observations of the Riedel peak, and a unified theory including both the gap-related rolloff and relaxation-time corrections will presumably be required to adequately explain the data.

Finally, it is of interest to compare our experimen-

tal results with a similar study by Clark and Lindelof³⁴ of the size of Josephson steps induced on the I - V curves of indium microbridges close to T_c by radiation at lower (microwave) frequencies. The voltage (frequency) dependence of that data was normalized to $I_c R = (\pi/4)\Delta^2(T)/ek_B T$, which is substantially smaller than $2\Delta/e$ near T_c . When replotted in the form used here, the curves all have a broad peak with $I_1^{\max}/I_c \sim 0.4$ occurring at $eV/2\Delta$ of 0.2 or less, and they rolloff roughly like the TDGL curve for $\Gamma = 50$ as shown in Fig. 7. This premature cutoff (which did not allow observation of the singular behavior at the gap frequency) may be due to unexpectedly large relaxation-time effects as suggested by Clark and Lindelof,³⁴ or may be due to reduction of I_c due to Joule heating at higher voltages because of the less favorable cooling geometry of bridges, as suggested by Octavio.³⁵

In summary, our experimental measurements of the frequency dependence of the ac Josephson effect in selected Nb point contacts at far-ir frequencies show that its strength increases at the gap frequency and rolls off beyond the gap frequency in qualitative agreement with the Werthamer theory. The quantitative discrepancies (of the order of a factor of 2 in the absolute size of the steps after correction for noise rounding) may be a result of the nonzero relaxation time of the order parameter in the point contact.

ACKNOWLEDGMENTS

We would like to thank Dr. D. T. Hodges for numerous useful suggestions concerning the far-ir laser. Discussions with Dr. R. E. Harris and Dr. D. G. McDonald were very helpful. R. Tobin performed the analog simulations. This work was supported by the Joint Services Electronics Program and the Office of Naval Research, with additional equipment funds from the NSF. One of us (D.A.W.) was supported by a Postgraduate Scholarship from the National Research Council of Canada.

*Present address: Exxon Research and Engineering Co., P. O. Box 45, Linden, N. J. 07036.

¹J. E. Zimmerman, Proceedings of the Applied Superconductivity Conference, Annapolis, 1972, IEEE Publication No. 72CH0682-5-TABSC, New York (unpublished), p. 544.

²M. Tinkham, M. Octavio, and W. J. Skocpol, J. Appl. Phys. **48**, 1311 (1977).

³D. A. Weitz, W. J. Skocpol, and M. Tinkham, J. Appl. Phys. **49**, 4873 (1978).

⁴D. A. Weitz, W. J. Skocpol, and M. Tinkham, Appl. Phys. Lett. **31**, 227 (1977).

⁵D. A. Weitz, W. J. Skocpol, and M. Tinkham, Phys. Rev. Lett. **40**, 253 (1978).

⁶B. D. Josephson, Phys. Lett. **1**, 251 (1962); Adv. Phys. **14**, 419 (1965).

⁷R. E. Harris, Phys. Rev. B **10**, 84 (1974).

⁸S. Shapiro, A. R. Janus, and S. Holly, Rev. Mod. Phys. **36**, 223 (1964).

⁹N. R. Werthamer, Phys. Rev. **147**, 255 (1966).

¹⁰C. A. Hamilton, Phys. Rev. B **5**, 912 (1972).

¹¹E. Riedel, Z. Naturforsch. A **19**, 1634 (1964).

¹²S. A. Buckner and D. N. Langenberg, J. Low Temp. Phys. **22**, 569 (1976).

¹³B. Kofoed and K. Saermark, Phys. Lett. **55A**, 72 (1975).

¹⁴G. Vernet and R. Adde, Appl. Phys. Lett. **28**, 559 (1976); H. Thome and Y. Couder, J. Appl. Phys. **49**, 1200 (1978).

¹⁵D. J. Scalapino and T. M. Wu, Phys. Rev. Lett. **17**, 315

- (1966).
- ¹⁶D. E. McCumber, J. Appl. Phys. **39**, 3113 (1968); W. C. Stewart, Appl. Phys. Lett. **12**, 277 (1968).
 - ¹⁷P. Russer, J. Appl. Phys. **43**, 2008 (1972).
 - ¹⁸V. Ambegaokar and A. Baratoff, Phys. Rev. Lett. **10**, 486 (1963); **11**, 104 (1963); L. G. Aslamasov and A. I. Larkin, JETP Lett. **9**, 87 (1969).
 - ¹⁹D. G. McDonald, E. G. Johnson, and R. E. Harris, Phys. Rev. B **13**, 1028 (1976).
 - ²⁰R. E. Harris, Phys. Rev. B **13**, 3818 (1976).
 - ²¹R. E. Harris, J. Appl. Phys. **48**, 5188 (1977).
 - ²²J. W. Dozier and J. D. Rodgers, IEEE Trans. Microwave Theory Tech. **MTT-12**, 360 (1964); **MTT-12**, 572 (1964) (E).
 - ²³D. A. Weitz, W. J. Skocpol, and M. Tinkham, Appl. Opt. **3**, 13 (1978).
 - ²⁴D. A. Weitz, W. J. Skocpol, and M. Tinkham, Proceedings of the Third International Conference on Submillimeter Waves and Their Applications, Guildford, England (1978), Infrared Phys. (to be published).
 - ²⁵C. A. Hamilton, Rev. Sci. Instrum. **43**, 445 (1972).
 - ²⁶M. Octavio, W. J. Skocpol, and M. Tinkham, IEEE Trans. Magn. **MAG-13**, 739 (1977).
 - ²⁷R. F. Broom, J. Appl. Phys. **47**, 5432 (1976).
 - ²⁸M. J. Stephen, Phys. Rev. **182**, 531 (1969); **186**, 393 (1969); P. A. Lee, J. Appl. Phys. **42**, 325 (1971).
 - ²⁹W. H. Henkeis and W. W. Webb, Phys. Rev. Lett. **26**, 1164 (1971).
 - ³⁰The data point for $eV/2\Delta \approx 0.94$ (233- μ m line) in Fig. 3 of Ref. 5 was based on preliminary data. Subsequent, more complete data yields a higher value shown in Fig. 7 of this paper.
 - ³¹K. K. Likharev and L. A. Yakobsen, Zh. Eksp. Theor. Fiz. **68**, 1150 (1975) [Sov. Phys. JETP **41**, 570 (1976)].
 - ³²L. Kramer and A. Baratoff, Phys. Rev. Lett. **38**, 518 (1977).
 - ³³B. R. Fjordbøge and P. E. Lindelof, J. Low Temp. Phys. **38**, 83 (1978).
 - ³⁴T. D. Clark and P. E. Lindelof, Phys. Rev. Lett. **37**, 368 (1976).
 - ³⁵M. Octavio, Technical Report No. 13 (Tinkham Series), Division of Applied Sciences, Harvard University, 1978 (unpublished), pp. 138-139.